

Tuning the exchange bias by using Cr interfacial dusting layers

Yu. Yanson, O. Petravic, K. Westerholt, and H. Zabel*

Institut für Experimentalphysik/Festkörperphysik, Ruhr-Universität Bochum, D-44780 Bochum, Germany

(Received 15 August 2008; revised manuscript received 24 October 2008; published 21 November 2008)

Exchange biased Fe/CoO bilayers with a Cr spacer layer between Fe and CoO layers have been studied using magnetometry. The Cr “dusting” layer thickness was varied between 0 and 10 Å. Independent of the growth method we find that the coercive field H_c drops much faster than the exchange bias field H_{eb} as a function of increasing Cr thickness. We attribute this effect to a rapid decoupling between the Fe and CoO layers with increasing Cr thickness. First, Cr decorates the grain boundaries on top of the CoO layer and screens the pinning centers for ferromagnetic domain walls. On further increasing the nominal Cr thickness the surface of the CoO grains is covered, which leads to a weakening of the exchange interactions at the interface and thus of H_{eb} . Furthermore, we show that the effect of the Cr-dusting layer on the system is insensitive upon the variation of the CoO-layer stoichiometry, whereas H_{eb} and H_c of the Cr-free CoO/Fe system vary significantly.

DOI: [10.1103/PhysRevB.78.205430](https://doi.org/10.1103/PhysRevB.78.205430)

PACS number(s): 75.60.Ej, 75.50.Ee, 78.70.Dm

I. INTRODUCTION

In magnetic heterostructures composed of a ferromagnetic (F) layer and an antiferromagnetic (AF) layer that share a common interface, an exchange bias (EB) can be observed below the blocking temperature of the AF.¹ This effect results in a shift of the hysteresis loop along the magnetic-field axis corresponding to an exchange bias field H_{eb} and is often accompanied by an enhancement of the coercivity H_c of the system. The effect has been extensively studied in the past because of its crucial importance in the design of spin-valve devices. A number of theoretical models have been proposed for the explanation of the phenomenon, but none of them is universal as to explain all details of the effect that accompany EB (for reviews we refer to Refs. 2–5). For example, it is well known that the F/AF interface plays an important role in the EB systems, but it is still unclear how the H_c enhancement is correlated with the H_{eb} .

Dusting the F/AF interface by a magnetic or nonmagnetic so-called δ layer of varying thickness is one possibility to modify the exchange interactions between F and AF. It has recently been demonstrated on systems with a nonmagnetic layer N at the F/AF interface that the exchange interaction responsible for EB between the F and AF is not a next-neighbor interaction, as is considered in most EB models, but is rather of long-range nature.⁶ However, controversial results on the dependence of H_{eb} on the N layer thickness can be found in the literature. It has been observed that in a CoO/noble metal/Py (Py= $\text{Ni}_{0.81}\text{Fe}_{0.19}$) system the exchange bias field decays exponentially with increasing thickness of the N layer.⁷ The decrease has been characterized by a decay length L , which depends on the N material and was determined to be of the order of 10 Å. On the other hand, in IrMn/N/FeCo systems, a much faster suppression of the EB was observed.⁷ Moreover, it was found that this suppression is relatively independent of the N material. Several groups have also studied the submonolayer thickness range of N layers on the EB effect. Mewes *et al.*⁸ reported on the observation of an oscillatory coupling in a FeMn/N/FeNi system similar to the interlayer exchange coupling observed in

F/N/F systems, with the first oscillation of H_{eb} occurring at a thickness below one monolayer of N . However, for interlayer exchange coupling in F/N/F systems, usually oscillation periods of at least two monolayers are found.⁹ Ali *et al.*¹⁰ recently reported on studies of the influence of submonolayer magnetic and nonmagnetic interface dusting layers on EB. They observed an increase of H_{eb} for most of the F dusting layers and a decrease for N layers. They explained their observations by the change of the magnetic configuration at the interface, leading to an increase or a decrease of the magnetic disorder, which in turn affects the EB. In the following we report on the effect that Cr-dusting layers have on the EB effect in the archetypical F metal/AF oxide interface. In particular we present our results on the Fe/Cr/CoO system for varying Cr layer thicknesses between 0 and 10 Å.

II. SAMPLE PREPARATION AND STRUCTURAL CHARACTERIZATION

The systems reported here have a layer sequence 50 Å Al/100 Å Fe/Cr spacer layer/400 Å CoO prepared on a Si(100) substrate with native oxide termination. We have studied two sets of samples. The first one was prepared using the ion-beam sputtering (IBS) technique. The base pressure in the chamber was approximately 5×10^{-9} mbar and the working pressure 4×10^{-3} mbar of Ar. The CoO layer was prepared using reactive sputtering of Co in oxygen, with the oxygen pressure being varied between 10^{-6} and 10^{-4} mbar by means of a high-precision valve. Care was taken that Cr and Fe, sputtered after CoO deposition, were not oxidized. All layers were prepared at room temperature. Since Cr wedge layers could not be grown in the ion-beam sputtering machine, four to six samples for each Cr spacer layer thickness were prepared and magnetically characterized. Their magnetic properties were averaged to eliminate the variation of the properties due to random effects. The standard deviation in H_{eb} and H_c was approximately 10%–15% for thin Cr layers (0.6–2 Å) and decreased to 3%–5% for thicker ones.

In the second set of samples, the CoO layers were reactively sputtered using IBS on a 40 mm long Si substrate.

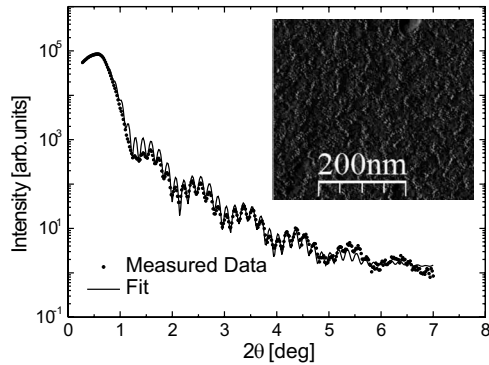


FIG. 1. X-ray reflectivity measurement of a typical Pd/Fe/Cr/CoO/SiO₂/Si sample (dots). The solid line shows a fit to the data points using the Parratt formalism (Ref. 11). The roughness of all layers in the system is below 3 Å, as obtained from the fit. The same roughness is also obtained from the AFM measurements of CoO surface (inset). In addition, polycrystalline grain boundaries can be seen in the AFM picture.

Afterwards the samples were transferred into a molecular-beam epitaxy (MBE) chamber, where a Cr wedge and a uniform Fe layer were deposited. Before deposition, no further treatment of the CoO surface was conducted. The wedge was created using the natural particle flow gradient of the effusion cell. A Pd layer was deposited as a cap layer to protect the system from oxidation. For structural and magnetic characterizations the samples were sliced into 1 mm wide stripes along the wedge direction. Since the thickness gradient of the wedge is very small, the Cr layer thickness can be assumed to be uniform within any one slice.

The layer structure and the interface structure were studied using x-ray scattering and atomic force microscopy (AFM). Typical examples for x-ray reflectivity measurements of the layer stack and for AFM images of the CoO surface are shown in Fig. 1. Both confirm an extremely low interface roughness between different layers and low surface roughness. The mean roughness amounts to less than 3 Å. Also, AFM images after Cr deposition did not show any increase of the roughness, which points to a smooth growth of the Cr layer. High angle x-ray diffraction measurements showed that the structure of the system is polycrystalline with no preferable grain orientation and a mean grain size of approximately 500 Å. The polycrystalline structure is also supported by the absence of magnetic anisotropy in samples, as has been measured using magneto-optic Kerr effect (MOKE) at room temperature. Grain boundaries can also be observed in the AFM image of the CoO surface (see inset Fig. 1). From the structural analysis of both sets we conclude that there is no significant difference between them.

III. MAGNETIC CHARACTERIZATION

A. Blocking temperature and training effect

Magnetic hysteresis loops were measured using a superconducting quantum interference device (SQUID) magnetometer (MPMS, Quantum Design). At room temperature, i.e., above $T_N=292$ K of CoO, the samples show no EB and H_c

amounts to 25 Oe. The hysteresis loop is rounded and the remanent magnetization is about 50% of the saturation magnetization, indicative of a multidomain state at remanence. All samples were cooled from 310 K in an external magnetic field of 3000 Oe, which is sufficient to saturate the magnetization of the Fe layer. The magnetization of the samples was measured along the field cooling direction that defines the unidirectional anisotropy axis at a temperature of 10 K. Typical hysteresis loops for different Cr layer thicknesses are shown in Fig. 2 for the first set of samples. The loops are shifted along the field axis toward negative field values, as expected for EB systems. For the samples with Cr layer thickness $t_{Cr}=0$ Å the shift equals to $H_{eb} \approx 325$ Oe. The coercivity, which is defined as the half width of the hysteresis loop at $M=0$, is dramatically enhanced from 25 Oe at room temperature to 540 Oe at 10 K. The hysteresis loop has perfect square shape, as typical for a film with strong uniaxial anisotropy. The sharp switching of the hysteresis at H_c indicates domain-wall nucleation and domain-wall motion as the dominating reversal mechanism. With Cr dusting the hysteresis loops in Fig. 2 essentially keep their perfect rectangular shape. However, one notices a strong drop of the coercive field so that the entire loop is shifted to negative field values.

For several values of t_{Cr} we have tested whether the samples show any “training” effect, i.e., a reduction of H_{eb} and H_c after repeated cycling in a magnetic field.²⁻⁵ We find that the training effect is rather small, namely, about 6% of H_{eb} and is independent on t_{Cr} . The shape of the hysteresis loop does not change after the first magnetization reversal.

Measurements of the temperature dependence of H_{eb} and H_c show no significant difference for different t_{Cr} (Fig. 3). The blocking temperature, i.e., the temperature of the onset of EB, is about 240 K, which is typical for nonepitaxial Fe/CoO interfaces.¹² Furthermore, the blocking temperature does not depend on the thickness of the Cr spacer layer. Thus, the blocking temperature is a parameter intrinsic to the AF layer rather than to the exchange coupling across the interface.

B. Cr thickness dependence

With increasing Cr thickness t_{Cr} we observe a rapid decrease of both H_{eb} and H_c for samples from the first series, as can be seen in Fig. 4. For thicknesses above one monolayer of Cr, i.e., $t_{Cr} \geq 1.44$ Å, H_{eb} can be well described by an exponential decay

$$H_{eb} \propto e^{-t_{Cr}/L}, \quad (1)$$

where L is the decay length of the exchange interaction across the spacer layer.⁶ The same fit has been used in Ref. 7 for other spacer layer materials. Typical values for the decay length, obtained by these authors, are about 2 Å. We find a decay length of $L=2.5 \pm 0.4$ Å, which is in good agreement with previous results.

An interesting effect is observed in the submonolayer thickness range of Cr. The coercive field decays extremely fast, dropping down to a value that is defined almost entirely by the F layer and not by the exchange bias to the AF. For $t_{Cr} > 1.44$ Å the coercive field remains nearly constant,

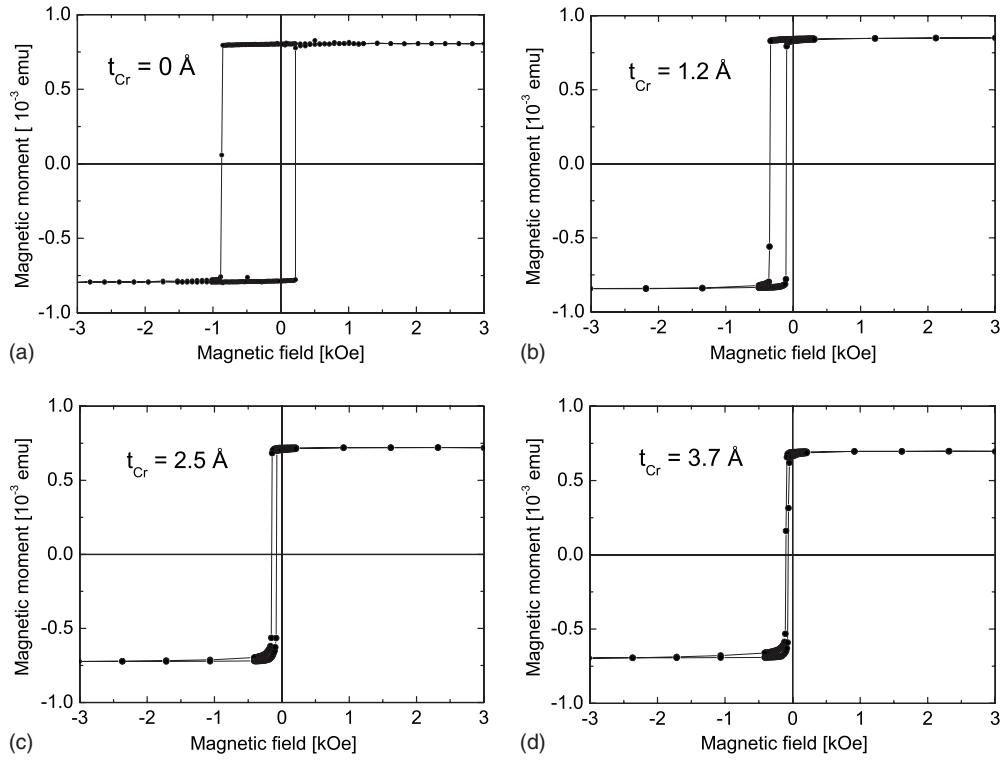


FIG. 2. Hysteresis curves of the samples at $T=10$ K with different t_{Cr} as given in the figure.

whereas H_{eb} decreases continuously. However, in the submonolayer thickness range, H_{eb} decays much slower with increasing Cr thickness than H_c .

In order to shed more light on the EB properties in the Cr submonolayer range, the second series of samples was studied. Though the sample preparation via IBS and MBE differs fundamentally, and in spite of the fact that the vacuum is broken for a short period of time for the sample transfer, samples prepared by both methods show similar dependencies of H_{eb} and H_c on t_{Cr} (Fig. 5): again H_c decreases much faster than H_{eb} in the submonatomic region of t_{Cr} .

C. Oxygen pressure dependence

The decrease of H_{eb} and H_c with increasing Cr thickness reported in the previous section could possibly be explained by a chemical reaction of Cr with CoO. If the 1:1 stoichiometry between cobalt and oxygen is not fulfilled, Cr may react with CoO and saturate free oxygen bonds. To check this possibility, we have varied the oxygen pressure during the sputtering process of CoO for several samples, while the other parameters were kept constant.

The pressure dependence of H_{eb} and H_c of the CoO/Fe samples without a Cr spacer layer is shown in Fig. 6. Both fields show a rapid variation with increasing oxygen pressure. The smallest EB field is observed for an oxygen pressure of 10^{-5} mbar O_2 . From x-ray Bragg scans and from measurements of the blocking temperature we confirmed that the minimum corresponds to an almost ideal 1:1 stoichiometry of Co and O in the CoO layer. The dependence at higher or lower pressures is in agreement with earlier results by Miltényi *et al.*¹³ and can be explained in the framework of the domain state model for the EB effect,^{13,14} viz., increasing the amount of oxygen atoms in CoO creates nonmagnetic

The pressure dependence of H_{eb} and H_c of the CoO/Fe samples without a Cr spacer layer is shown in Fig. 6. Both fields show a rapid variation with increasing oxygen pressure. The smallest EB field is observed for an oxygen pressure of 10^{-5} mbar O_2 . From x-ray Bragg scans and from measurements of the blocking temperature we confirmed that the minimum corresponds to an almost ideal 1:1 stoichiometry of Co and O in the CoO layer. The dependence at higher or lower pressures is in agreement with earlier results by Miltényi *et al.*¹³ and can be explained in the framework of the domain state model for the EB effect,^{13,14} viz., increasing the amount of oxygen atoms in CoO creates nonmagnetic

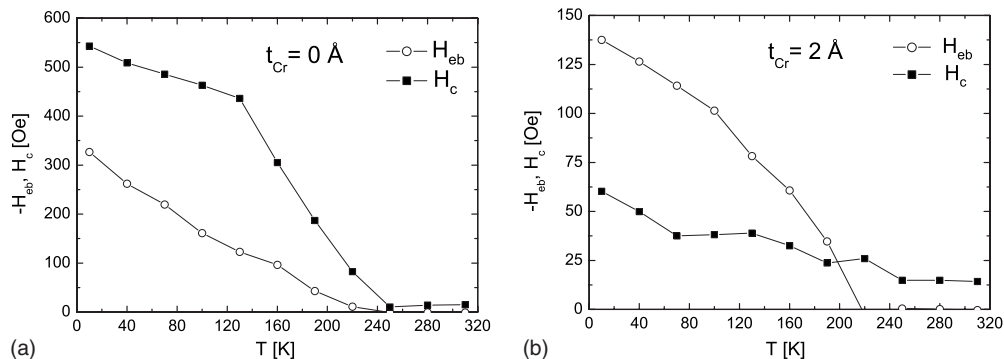


FIG. 3. Temperature dependence of H_{eb} and H_c of samples with (a) $t_{Cr}=0$ Å and (b) $t_{Cr}=2$ Å.

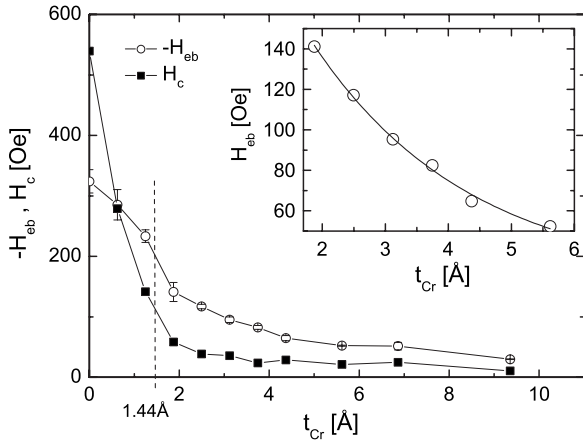


FIG. 4. Dependence of H_{eb} and H_c on t_{Cr} for samples prepared by ion-beam sputtering. The dashed vertical line corresponds to the nominal thickness of a monatomic layer of Cr. Inset shows a fit to the data points of H_{eb} for Cr thicknesses above one monolayer using Eq. (1).

defects in the grains that act as pinning centers for the domain walls in the AF. Consequently the number of AF domains increases, leading to an increase of uncompensated spins at the interface. The increase of EB at lower oxygen pressures occurs because of the creation of ferromagnetic Co clusters in the CoO layer. This assumption is supported by the observation of ferromagneticlike hysteresis curves above the Néel temperature of CoO in samples containing only CoO films. Thus the exchange bias not only acts at the CoO/Fe interface, but also between CoO and Co clusters. Also the presence of underoxidized $CoO_{1-\delta}$ ($\delta > 0$) could contribute to the enhancement of H_{eb} , as it has been recently shown in Ref. 15.

Next we discuss the dependence of H_{eb} and H_c on the O_2 pressure during the CoO deposition and subsequent Cr deposition for different thicknesses t_{Cr} in the submonolayer region as seen in Fig. 7. Three different sample series were prepared at a pressure of 1×10^{-5} , 2×10^{-5} , and 5.4×10^{-5} mbar O_2 .

If excess oxygen was the reason for the peculiar dependence of H_{eb} and H_c on t_{Cr} , then both fields should sensitively depend on the O_2 pressure at which the CoO layer is

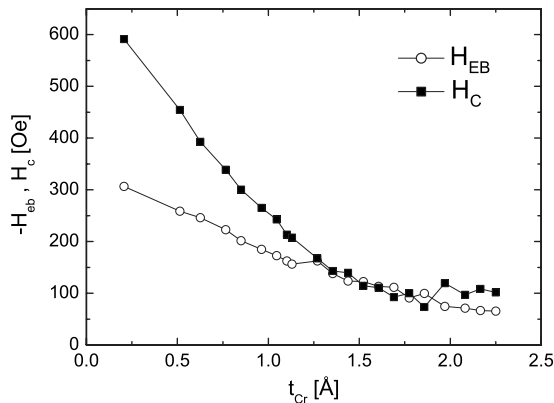


FIG. 5. Thickness dependence of H_{eb} and H_c measured at $T = 10$ K for Cr and Fe metal films grown by molecular-beam epitaxy.

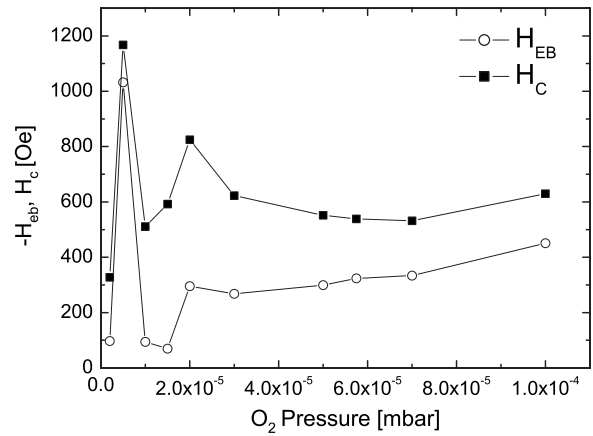


FIG. 6. Dependence of the exchange bias field (circles) and the coercive field (squares) on the oxygen pressure during the CoO-layer deposition in samples without a Cr interface layer.

prepared. However, this is not the case as can be seen in Fig. 7. As mentioned above, H_c drops fast with increasing t_{Cr} , whereas H_{eb} exhibits a much slower t_{Cr} dependence, independent of the oxygen pressure. In detail, the dependence of the EB field for pressures 2×10^{-5} mbar and higher is very similar. But samples prepared at 1×10^{-5} mbar have a much smaller H_{eb} that drops to almost zero with increasing Cr thickness beyond one monolayer. From these observations we can conclude that possible oxygen excess during CoO preparation is not the cause for the t_{Cr} dependence of H_{eb} and H_c .

IV. DISCUSSIONS

We have seen in the previous sections that the coercive field drops much faster with increasing Cr-dusting layer thickness at the Fe/CoO interface than the exchange bias field. Furthermore, we notice that the general properties of H_{eb} and H_c do not depend on the oxygen pressure during the CoO preparation, indicating that the defect structure of the AF layer has a quantitative but no qualitative effect on the overall behavior of the exchange bias effect.

Considering first the coercive field, the network of grain boundaries in the polycrystalline AF film extends over an area larger than the domain-wall width of the F layer. In Fig. 1 (inset) it can be found that the grain boundaries form lines of several hundreds of nanometers in length. Assuming that the grain boundaries represent the magnetically most distorted parts of the AF layer, they create pinning centers for domain walls in the F layer, which, in turn, enhance the coercivity of the system below the blocking temperature. Thus we may conclude that the grain boundaries of the AF layer are mostly responsible for the measured H_c at 10 K.

As the sputtered Cr atoms reach the CoO surface with some kinetic energy, they diffuse on the surface and finally settle into local potential minima. On polycrystalline surfaces the energetically deepest and laterally broadest potential minima are the grain boundaries in the AF layer. Thus one would expect that the sputtered Cr atoms would first preferably “fill” in the grain boundaries, thus screening their

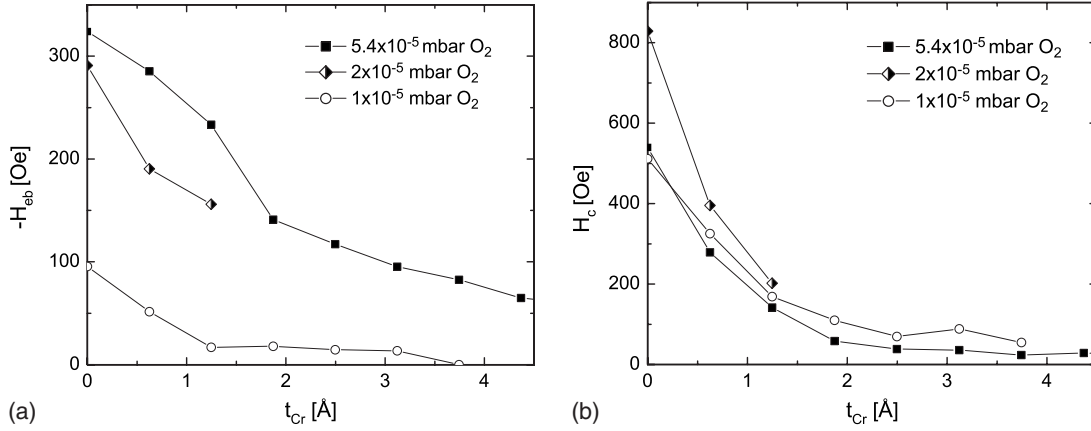


FIG. 7. Comparison of the thickness dependence of (a) H_{cb} and (b) H_c for the samples, prepared at $p_{O_2} = 5.4 \times 10^{-5}$ mbar (filled symbols), 2×10^{-5} mbar (half-filled symbols), and at 1×10^{-5} mbar (open symbols).

influence on the domain-wall motion in the F layer. The screening length of about 2.5 \AA correlates well with the roughness of the CoO surface, determined with AFM, and the roughness of the F/AF interface determined by x-ray reflectivity. Grain boundaries on the CoO surface then correspond to the magnetically most frustrated regions. Consequently, the screening effect of Cr can be considered as a reduction of the magnetic frustration, which the Fe layer “senses” in the vicinity of Fe/CoO interface. This then leads to a rapid suppression of H_c .¹⁶

Considering the exchange bias field, we suggest that H_{cb} mostly depends on the direct interfacial contact between the F layer and the bulk of the AF grains. The oxygen dependence can well be explained by the domain state model for EB.¹⁴ It also explains the fact that H_{cb} is barely sensitive to the deposition of small amounts of Cr on the interface that tend to accumulate first at the grain boundaries. Further deposition of Cr covers the whole interface, screening not only the effect of the AF grain boundaries on the H_c , but also the effect of the AF grains on H_{cb} , thus finally leading to a decrease of both H_{cb} and H_c with increasing Cr thickness. Cr as an antiferromagnetic transition metal could, in principle, mediate the exchange bias between the Fe and the CoO layers. While Cr is well known to provide strong interlayer exchange coupling,^{9,17,18} it is also well known that Cr weakens the exchange bias coupling.¹⁹ In case of a structurally disordered and polycrystalline Cr interfacial layer the mediating exchange bias effect can safely be neglected.

Recently, Radu *et al.*²⁰ showed that interface spin disorder is the main reason for the discrepancy between model calculations on the relation between H_{cb} and H_c and experimental results. However, taking into account spin disorder at the interface between the F and the AF layer by modifying the well-known Meiklejohn and Bean (MB) model,¹ an almost perfect agreement can be reached. In this model it is assumed that the interface anisotropy depends on the quality of the interface and leads to an enhanced coercivity. When K_{eff} is zero, the system behaves ideally as described by the MB model,¹ i.e., the coercive field is zero and the exchange bias field is finite. In the other case, i.e., when the interface is disordered, the effective anisotropy is related to the available interfacial coupling energy following $K_{eff} = (1 - f)J_{EB}$, where

J_{EB} is the total exchange energy of an ideal system without additional coercivity. With this assumption the absolute value of the EB field is reduced by the factor f as compared to the MB model. Thus the factor f describes the conversion of interfacial energy into coercivity through rotation of interfacial AF spins. In this model, H_{cb} and H_c are intimately related, i.e., a large exchange bias field results in a small coercive field and vice versa. This model works very well for the CoFe/IrMn system, as shown in Ref. 20. However in the present Fe/Cr/CoO system the weakening of the exchange bias field with increasing Cr thickness does not lead to an increased coercivity. Instead, the coercivity drops even faster than the exchange bias field. From this we can conclude that the Cr-dusting layer decouples the F and AF layers fast and very effectively and that a conversion from exchange energy into enhanced spin rotation at the interface does not take place.

V. SUMMARY AND CONCLUSION

We have studied in detail the effect of a Cr-dusting layer at the interface of Fe and CoO on the exchange bias effect at low temperature. Two sample series were grown by ion-beam sputtering and by molecular-beam epitaxy. In both sample series the F and the AF layers are polycrystalline by the choice of an amorphous Si/SiO₂ substrate. Independent of the growth method chosen, the same overall effect was observed by SQUID hysteresis measurements after field cooling to 10 K. With increasing Cr thickness the coercive field drops rapidly and much faster than the exchange bias field. The screening length of the exchange bias field was determined to be about 2.5 \AA . We attribute this effect to a preferential accumulation of Cr at the grain boundaries of the polycrystalline CoO layer, thereby effectively screening the pinning centers for domain-wall motion. Increasing the Cr thickness further, also the exchange bias at the F/AF interface is gradually screened since Cr does not mediate the exchange bias between Fe and CoO. We have also studied the effect of oxygen pressure during CoO growth on the exchange bias with and without Cr-dusting layer. The variation with the oxygen pressure, which controls the defect density in the CoO layer, changes the magnitude of the exchange

bias effect in accordance with the domain state model, but does not alter the overall behavior.

Concluding, dusting of the F/AF Fe/CoO interface with Cr ultrathin films not only contributes to the detailed understanding of the exchange bias effect, but also allows us to tune exchange bias fields and coercive fields to specified values. This may have important implications for the design of spin-valve systems.

ACKNOWLEDGMENTS

We would like to thank P. Stauche, J. Podschwadek, and S. Erdt-Böhm for technical support. This work was supported by SFB 491 of the Deutsche Forschungsgemeinschaft: “Magnetic Heterostructures: Spinstructure and Spintransport,” which is gratefully acknowledged.

*hartmut.zabel@ruhr-uni-bochum.de

¹W. H. Meiklejohn and C. P. Bean, *Phys. Rev.* **105**, 904 (1957).

²J. Nogués and I. K. Schuller, *J. Magn. Magn. Mater.* **192**, 203 (1999).

³A. Berkowitz and K. Takano, *J. Magn. Magn. Mater.* **200**, 552 (1999).

⁴R. Stamps, *J. Phys. D* **33**, R247 (2000).

⁵R. Radu and H. Zabel, *Springer Tracts Mod. Phys.* **227**, 97 (2007).

⁶N. J. Gökemeijer, T. Ambrose, and C. L. Chien, *Phys. Rev. Lett.* **79**, 4270 (1997).

⁷L. Thomas, A. J. Kellock, and S. S. P. Parkin, *J. Appl. Phys.* **87**, 5061 (2000).

⁸T. Mewes, B. F. P. Roos, S. O. Demokritov, and B. Hillebrands, *J. Appl. Phys.* **87**, 5064 (2000).

⁹B. Heinrich, *Springer Tracts Mod. Phys.* **227**, 185 (2007).

¹⁰M. Ali, C. H. Marrows, and B. J. Hickey, *Phys. Rev. B* **77**, 134401 (2008).

¹¹L. G. Parratt, *Phys. Rev.* **95**, 359 (1954).

¹²G. Nowak, A. Remhof, F. Radu, A. Nefedov, H.-W. Becker, and H. Zabel, *Phys. Rev. B* **75**, 174405 (2007).

¹³P. Miltényi, M. Gierlings, J. Keller, B. Beschoten, G. Güntherodt, U. Nowak, and K. D. Usadel, *Phys. Rev. Lett.* **84**, 4224 (2000).

¹⁴U. Nowak, K. D. Usadel, J. Keller, P. Miltényi, B. Beschoten, and G. Güntherodt, *Phys. Rev. B* **66**, 014430 (2002).

¹⁵J. Riveiro, P. Normile, J. D. Toro, T. Muñoz, P. Muñoz, J. González, and J. Andrés, *New J. Phys.* **10**, 083028 (2008).

¹⁶C. Leighton, J. Nogués, B. J. Jönsson-Akerman, and I. K. Schuller, *Phys. Rev. Lett.* **84**, 3466 (2000).

¹⁷P. Grünberg, *J. Phys.: Condens. Matter* **13**, 7691 (2001).

¹⁸H. Zabel, *J. Phys.: Condens. Matter* **11**, 9303 (1999).

¹⁹J. S. Jiang, G. P. Felcher, A. Inomata, R. Goyette, C. Nelson, and S. D. Bader, *Phys. Rev. B* **61**, 9653 (2000).

²⁰F. Radu, A. Westphalen, K. Theis-Bröhl, and H. Zabel, *J. Phys.: Condens. Matter* **18**, L29 (2006).